CrossMark

RESEARCH PAPER

A new rhynchosaur from south Brazil (Santa Maria Formation) and rhynchosaur diversity patterns across the Middle-Late Triassic boundary

Cesar Leandro Schultz[1] · Max Cardoso Langer[2] · Felipe Chinaglia Montefeltro[3]

Abstract The rhynchosaur previously referred to as the "Mariante Rhynchosaur" is here formally described as a new genus and species based on two specimens: a complete skull (without the lower jaw) articulated with the three first cervical vertebrae and a set of right maxilla and dentary. Both specimens were collected at the same site in Rio Grande do Sul, Brazil, from deposits of the Santa Maria Formation considered of Ladinian (Middle Triassic) age. Diagnostic characters include the contact between prefrontal and postfrontal, a pair of deep frontal grooves, and a very deep skull. A new phylogenetic analysis recovered the new taxon as a member of the Stenaulorhynchinae, a relatively diverse clade of Middle Triassic rhynchosaurs, with records in India, east Africa, and the Americas. Evidence suggests that the extinction of that clade took place in the context of a faunal turnover across the Ladinian-Carnian boundary, when it was replaced by the much more abundant Late Triassic hyperodapedontine rhynchosaurs.

✉ Max Cardoso Langer
  mclanger@ffclrp.usp.br

1 Departamento de Paleontologia e Estratigrafia, Instituto de Geociências, Universidade Federal do Rio Grande do Sul, Av. Bento Gonçalves 9500, Porto Alegre, RS 91540-000, Brazil

2 Departamento de Biologia, Faculdade de Filosofia Ciências e Letras de Ribeirão Preto, Universidade de São Paulo, Av. Bandeirantes 3900, Ribeirão Preto, SP 14040–901, Brazil

3 Departamento de Biologia e Zootecnia, Faculdade de Engenharia, Universidade Estadual Paulista, Passeio Monção 226, Ilha Solteira, SP 15385-000, Brazil

Kurzfassung Der früher als "Mariante Rhynchosaur" bezeichnete Rhynchosaurier wird hier, anhand zweier Exemplare (ein unterkieferloser kompletter Schädel mit den drei ersten Halswirbeln sowie ein Satz rechter Oberkiefer und Dentale), formell als neue Gattung und Art beschrieben. Beide Exemplare wurden in der selben Lagerstätte in Rio Grande do Sul, Brasilien, gefunden, in Ablagerungen der Santa Maria Formation aus dem Zeitalter des Ladinium (Mittlere Trias). Diagnostische Merkmale beinhalten den Kontakt zwischen Pre- und Postfrontale, ein Paar tiefer frontaler Furchen, und einen sehr tiefen Schädel. Eine neue phylogenetische Analyse positionierte das neue Taxon als Mitglied der Stenaulorhynchinae, eine relative vielfältige Klade an Rhynchosauriern des Mittleren Trias, mit Funden aus Indien, Ostafrika und den Amerikas. Hinweise deuten darauf, dass das Aussterben der Klade im Zusammenhang eines Faunenaustausches an der Ladinium-Karnium Grenze stattfand, als sie durch die viel häufigeren hyperodapedontinen Rhynchosaurier des Späten Trias ersetzt wurden.

Introduction

Rhynchosaurs are an exclusively Triassic group of herbivorous archosauromorphs. They have been recorded in most areas of Pangea, including what is now Brazil, Argentina, USA, Canada, England, Scotland, Tanzania, Zimbabwe, South Africa, Madagascar, and India (Langer et al. 2000). The oldest representatives of the group are Early Triassic in

2 Springer

age (Butler et al. 2015; Ezcurra et al. 2016) and various Middle and Late Triassic terrestrial faunas were dominated by rhynchosaurs as primary consumers (Langer 2005). Rhynchosaurs in Brazil have thus far been found only in the Santa Maria Formation (Triassic of the Paraná Basin), Rio Grande do Sul, where they represent about 80 % of the fossil specimens collected in the *Hyperodapedon* Assemblage Zone, Alemoa Member (Langer et al. 2007). Rhynchosaurs are, however, much rarer in the older *Dinodontosaurus* AZ, known only by the specimens described here (Schultz and Azevedo 1990). These correspond to the animal until now informally known as the "Mariante Rhynchosaur" (Langer and Schultz 2000a; Langer et al. 2007; Montefeltro et al. 2010, 2013; Mukherjee and Ray 2014; Butler et al. 2015), in reference to the town of Porto Mariante, near the site where the fossils were collected.

Phylogenetic analysis

The phylogenetic position of the "Mariante Rhynchosaur" within Rhynchosauria was examined based on a modified version of the data set of Ezcurra et al. (2016). In order to expand the sampling of Middle Triassic rhynchosaurs, two fragmentary forms have been added to the original data set: the North American *Ammorhynchus navajoi* from the Moenkopi Formation (Nesbitt and Whatley 2004) and *Mesodapedon kuttyi* from the Yerrapalli Formation, Indian subcontinent (Chatterjee 1980). Besides, as the inclusion of *Noteosuchus colletti* (*Lystrosaurus* Assemblage Zone, Induan of South Africa) in the original analysis resulted in a large politomy at the base of Rhynchosauria (Ezcurra et al. 2016), and because early rhynchosaurs are not the focus of this study, we deleted that taxon from the data set. We also added 12 characters (see Supplementary Material) based on newly recognized discrete morphological variations within the sampled taxa. Taxon scoring was based on first-hand examination of specimens, with the exception of *A. navajoi*, *M. kuttyi*, *Prolacerta broomi*, and *Protorosaurus speneri*. Data sources of each taxon are provided in the Supplementary Material. Multistate characters 63, 64, 70, 73, and 75 of the original analysis (Ezcurra et al. 2016) were dismembered into two characters each for contingent coding (see Supplementary Material), following the a hypothesis of nested homology (Brazeau 2011). The remaining multistate characters (i.e., 14, 60, and 76) were treated as non-additive, following non-nested homology hypotheses (Brazeau 2011). The final matrix, composed of 16 taxa and 112 characters (Supplementary Material), was analyzed using the software TNT version 1.1 (Goloboff et al. 2008) under the implicit enumeration algorithm, collapse of "zero-length" branches, having *Protorosaurus speneri* as the primary outgroup. In addition to consistency

(CI) and retention (RI) indices for the most parsimonious trees, we performed both standard and GC bootstrap analyses (1000 heuristic pseudoreplicates each) and calculated the decay index (Bremer 1994) for each node.

Systematic palaeontology

Rhynchosauria Osborn, 1903 (sensu Dilkes 1998).
Rhynchosauridae Cope, 1870 (sensu Dilkes 1998).
Hyperodapedontidae Lydekker, 1885 (sensu Langer and Schultz 2000b).
Stenaulorhynchinae Kuhn, 1933 (sensu Langer and Schultz 2000a).
Brasinorhynchus mariantensis gen. et sp. nov.

Etymology

The generic epithet is formed of the Portuguese word "brasino", used for red horses in south Brazil, and the Greek word rhynchos (= beak), in reference both to the color of the fossil and the gross resemblance of the holotype skull to that of a horse. The specific name refers to Porto Mariante, the nearest town to the type-locality.

Type material

Holotype—UFRGS-PV-0168-T, complete skull (lacking the lower jaw), atlas, axis and third cervical vertebra; paratype—UFRGS-PV-0315-T, right maxilla and dentary.

Type locality and horizon

The type specimens were collected at the same site (29°42′9.72″S; 51°54′58.01″W), along RS-240 road (Fig. 1) near the town of Porto Mariante, 28 km east of Venâncio Aires, municipality of Bom Retiro do Sul, Rio Grande do Sul, Brazil (Schultz and Azevedo 1990). This belongs to the Bom Retiro do Sul structural block of Da Rosa (2014). The type-locality ("Mariante 1"; Fig. 1) has yielded isolated dicynodont remains, whereas a nearby site ("Mariante 2"; Fig. 1) has yielded more complete specimens referable to the genus *Dinodontosaurus*. Accordingly, the Alemoa Member beds (Santa Maria Formation; Andreis et al. 1980) in the area are tentatively assigned to the *Dinodontosaurus* Assemblage Zone (Lucas 2001; Langer et al. 2007; Soares et al. 2011; Horn et al. 2014). Under a sequence stratigraphic framework, these deposits are included in the Santa Maria 1 Sequence of Zerfass et al. (2003), i.e., the Pinheiros-Chiniquá Sequence of Horn et al. (2014). In terms of age, the *Dinodontosaurus* Assemblage Zone is typically regarded as Ladinian (Abdala et al. 2009, 2013), but see age discussion at the end of the paper.
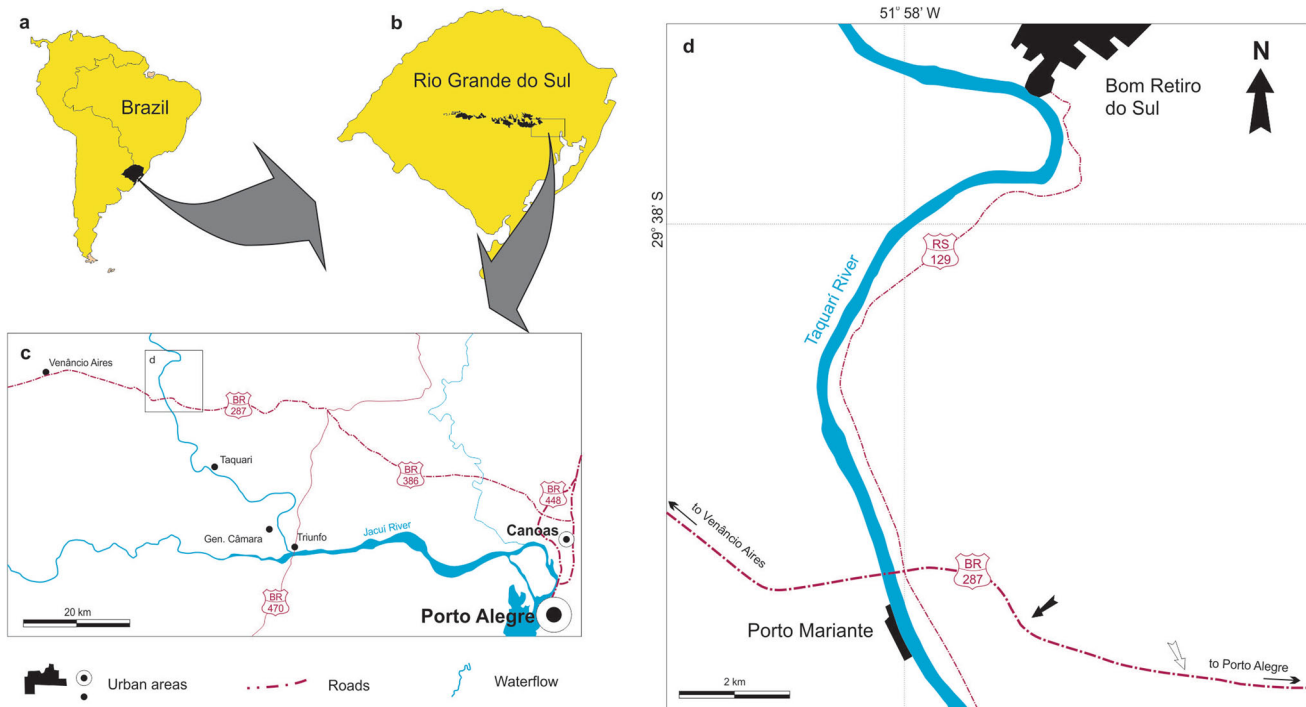
Fig. 1 Location of the type-locality of *Brasinorhynchus mariantensis* within South America (**a**), Brazil, and Rio Grande do Sul (**b**). *Black shading* in **b** represents surface distribution of the Alemoa beds (Santa Maria Formation); area depicted in **d** indicated in **c**; *white arrow* points to "Mariante 1" site, *black arrow* points to "Mariante 2" site

Diagnosis

Brasinorhynchus mariantensis is the only known rhynchosaur that possesses a prefrontal-postfrontal contact, excluding the frontals from the orbit. Its skull is also markedly deep, as reflected in the vertical elongation of bones/structures such as the premaxillae, supraoccipital, parasphenoid rostrum, and quadrate. The taxon is also unique for the very deep pair of grooves in the dorsal surface of the frontal, which converge towards the caudal margin of the bone; the presence of a well-marked 'V'-shaped crest along frontal-postfrontal contact, rostral to the margin of the supratemporal fossa; the presence of scattered foramina above the anguli oris crest; and a broad/rounded caudal process of the postorbital.

Institutional abbreviations UFRGS-PV: Vertebrate Paleontology collection of the Universidade Federal do Rio Grande do Sul, Porto Alegre-Brazil.

Description (Figs. 2, 3, 4, 5, 6, 7, 8, 9)

The bones are permineralized by calcite and partially covered by a thin layer of iron oxide. The holotype skull is lateromedially compressed, as it was found lying on its left side. Due to the compression, the premaxillae were shifted forwards, the nasals became somewhat bowed, projecting dorsally above the prefrontals, and the parietal was displaced relative to the dorsal ends of epipterygoid, prootic, and supraoccipital. The quadrate processes of the pterygoid were also displaced towards the midline, almost touching one another. The left lachrymal is fractured in the area where, in other rhynchosaurs, the lachrymal and infraorbital foramina are seen. Quadrate, quadratojugal, squamosal, and parts of the pterygoid were severely displaced on the left side, but moved only somewhat medially on the right side. The lateromedial compression also reduced the angle formed by the paraoccipital processes in dorsal view and the neurocranium was somewhat pulled rostrally. This also resulted in the double fracture of the right paraoccipital process, as it remained sutured to the squamosal. Nonetheless, the lateromedial compression alone does not account for the remarkable depth of the skull, which is considered a typical feature of the taxon.

The **premaxillae** are more robust than in other known rhynchosaurs, but their entire length is unknown. Both components of the pair are transversely broken, revealing a triangular cross-section with a smaller rostral margin. For approximately half of their preserved length, the premaxillae touch one another medially via a flat surface. They diverge proximally, bordering the single external naris rostrolaterally. In this portion, the cross-section of the bones are smaller and they fit into a slot formed at the maxilla/nasal contact.
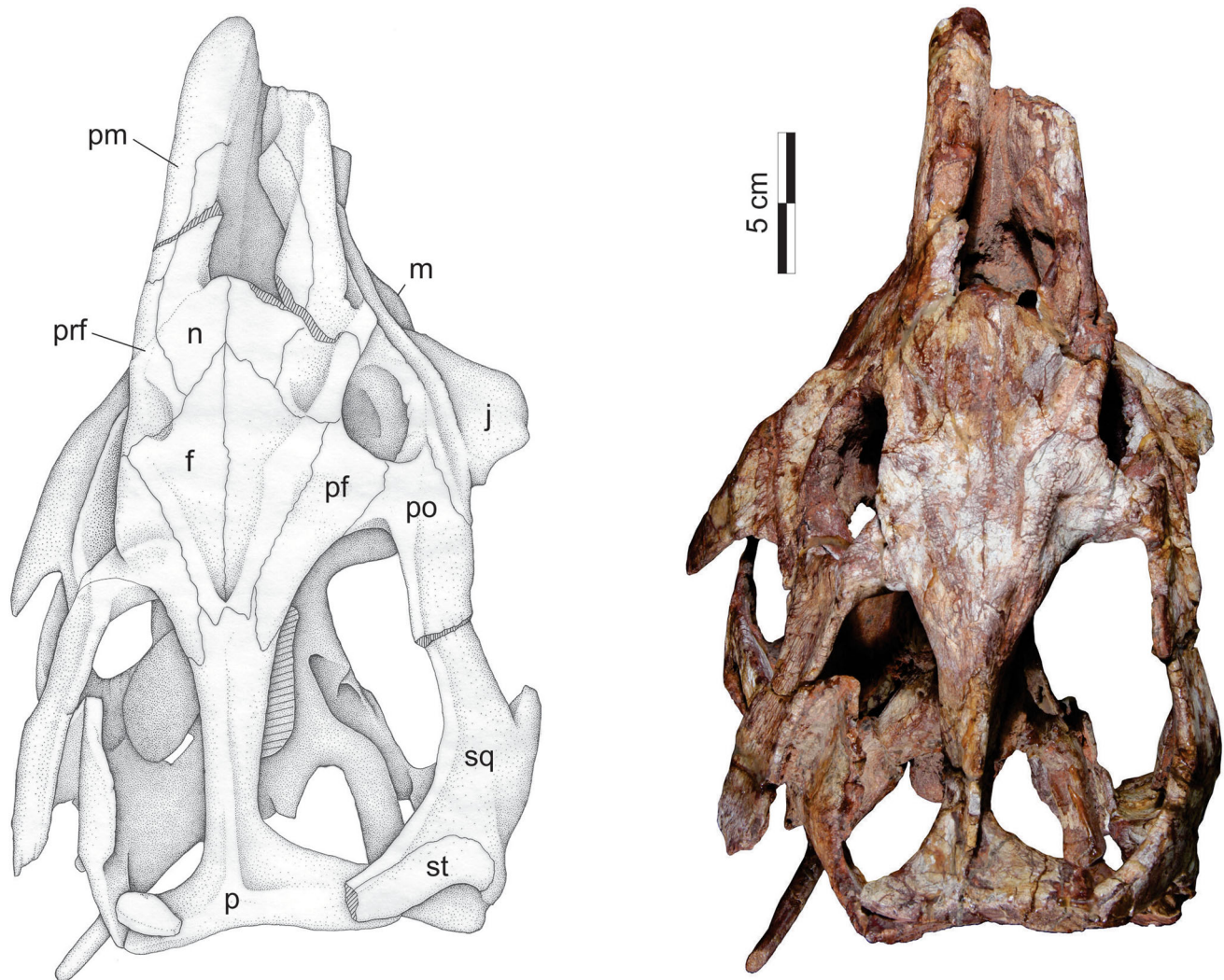
Fig. 2 *Brasinorhynchus mariantensis* (UFRGS-PV-0168-T; holotype). Drawing and photograph of the skull in dorsal view. *f* frontal, *j* jugal, *m* maxilla, *n* nasal, *p* parietal, *pf* postfrontal, *pm* premaxilla, *po* postorbital, *prf* prefrontal, *sq* squamosal, *st* supratemporal

The **maxilla** is crescent-shaped in lateral view, with a convex tooth-bearing ventral margin. Dorsally, the bone meets the premaxilla rostrally and prefrontal, jugal, and lachrymal caudally. Ventral to the premaxillary contact, the rostral margin of the maxilla bears a marked notch, as typical of many rhynchosaurs (Montefeltro et al. 2010). The jugal suture is curved and placed just rostral to the jugal anguli oris crest, which also extends briefly onto the lateral surface of the maxilla (Fig. 3). In ventral view, the maxilla is shaped as an elongated triangle, the medial and lateral margins of which are formed by two elongated crests. These are wedge shaped in cross section and bear small teeth. The space between the crests is deeply excavated and broad, especially on its caudal portion, where a third and feebler tooth-bearing crest is seen. The groove formed between this middle crest and the outer marginal crest is narrower and deeper than that formed with the inner

marginal crest. Both in the holotype skull and in the isolated maxilla UFRGS-PV-0315, the outer marginal crest bears teeth only along its apex, whereas these expand along the medial and lateral walls of the inner marginal crest. The two grooves are evident up to the caudal margin of the maxilla, where there is no occlusion with the dentary crests. Accordingly, the two grooves represent an inherent feature and were not produced by wear. The lateral groove is limited to the caudal half of the maxillary occlusal surface, whereas the medial groove extends to the rostral-most portion of that surface. The whole lingual surface of the maxilla is covered by numerous, small and packed lingual teeth, the crowns of which are worn out. The palatal surface of the maxilla meets the jugal and ectopterygoid caudally. Medially, it meets the vomer more rostrally and the palatine more caudally, forming the lateral margin of the choana between these.
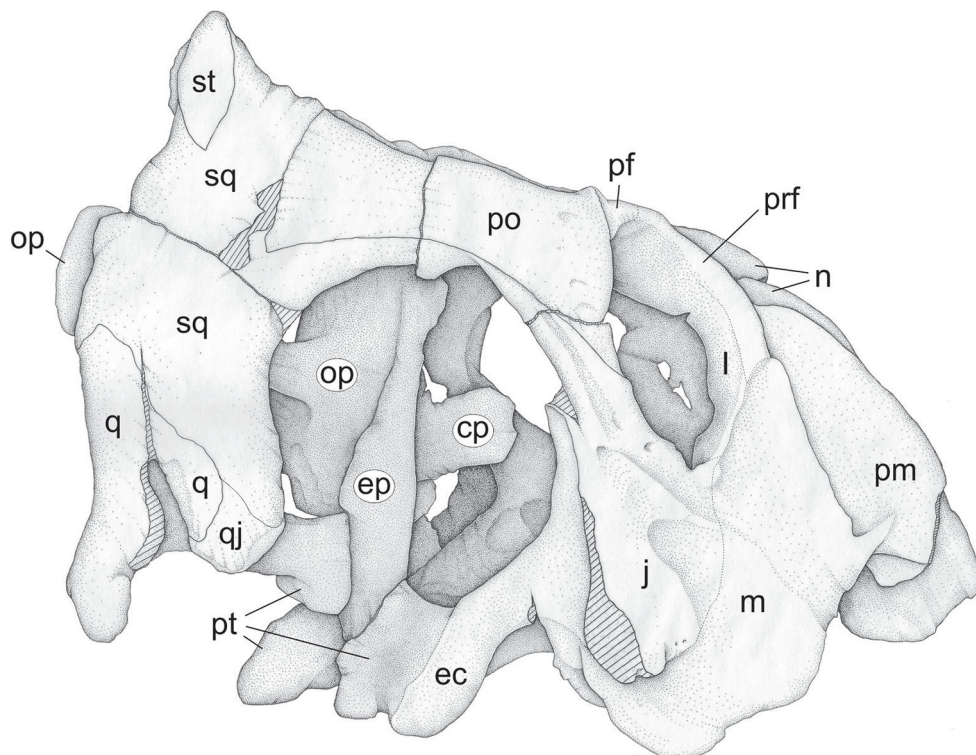
Fig. 3 *Brasinorhynchus mariantensis* (UFRGS-PV-0168-T; holotype). Drawing and photograph of the skull in left lateral view. *cp* cultriform process, *j* jugal, *l* lachrymal, *m* maxilla, *n* nasal, *op* opistotic, *p* parietal, *pf* postfrontal, *pm* premaxilla, *po* postorbital, *prf* prefrontal, *pt* pterygoid, *q* quadrate, *qj* quadratojugal, *sq* squamosal. *White arrow* indicates extension of the anguli oris crest onto the lateral surface of the maxilla
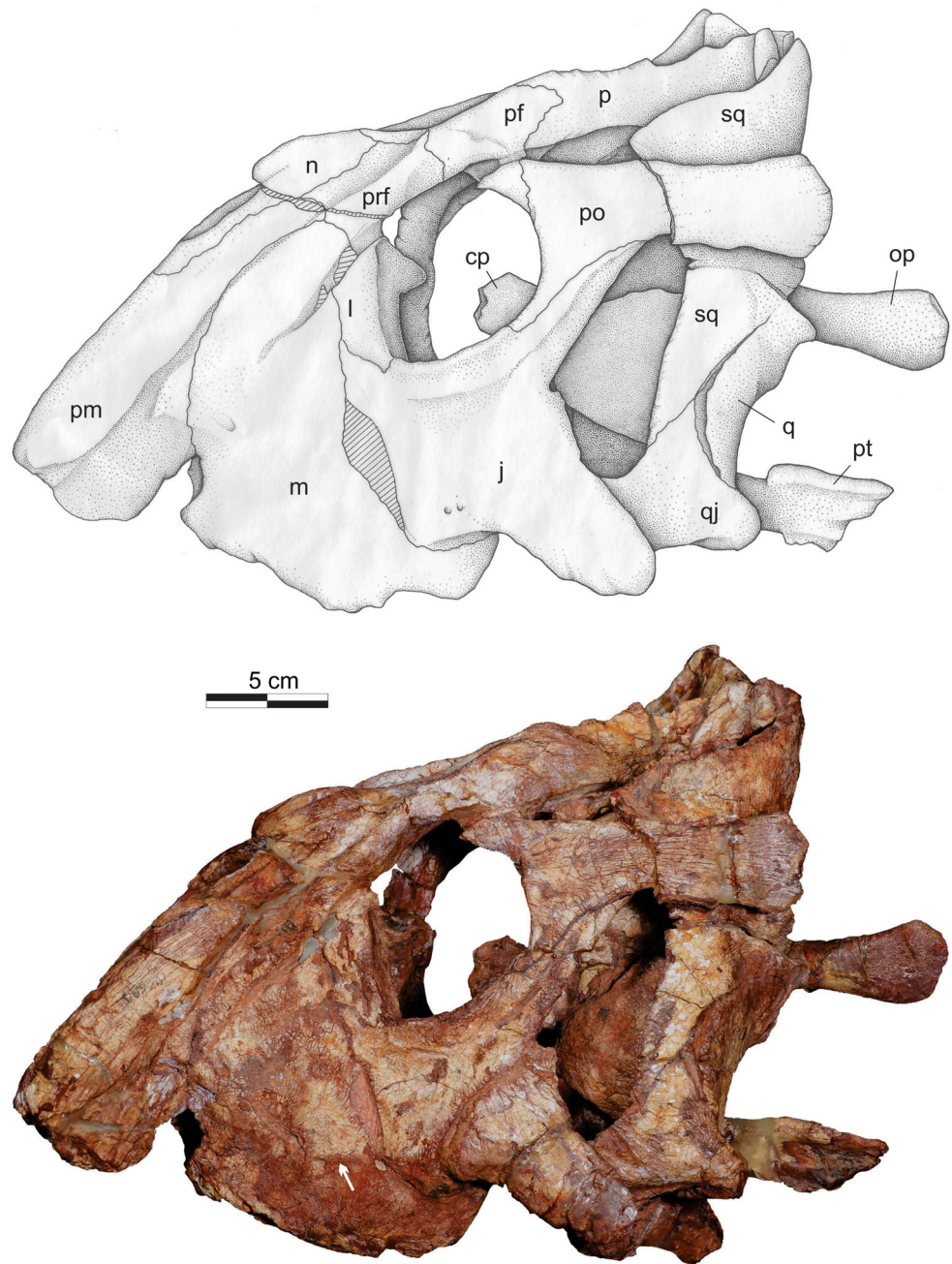
The rostral margin of the **nasals** forms the rounded caudal border of the external naris, with no evidence of an internarial bar. Each bone has a rhombic shape, with an elongate rostral process that extends parallel to the premaxilla, along the lateral margin of the naris. Caudally, there is a V-shaped suture that receives a wedge formed by the frontals. Each **frontal** has a roughly triangular shape, with the largest margin forming the midline contact with its counterpart. The rostrolateral margin meets nasal and prefrontal, whereas the caudolateral sutures with the postfrontal. This suture extends over a rounded crest that converges caudally to meet its pair. A recessed area is formed at the caudal region of the frontal, between the pair of ridges. Laterally, the frontals do not reach the margin of the orbit. The fused **parietals** form a "T" shaped element, where the length (corresponding to the intertemporal bar) is greater than the width (measured between the lateral tips of the caudal processes). The intertemporal bar presents a well-marked sagittal crest that is continuous to the ridges that mark the frontal-postfrontal contact, forming a "Y" shaped structure. Ventrally, the intertemporal bar is broader, meeting the epipterygoid, prootic, and

Fig. 4 *Brasinorhynchus mariantensis* (UFRGS-PV-0168-T; holotype). Drawing and photograph of the skull in right lateral view. *cp* cultriform process, *ec* ectopterygoid, *ep* epipterygoid, *j* jugal, *l* lachrymal, *m* maxilla, *n* nasal, *op* opistotic, *pf* postfrontal, *pm* premaxilla, *po* postorbital, *prf* prefrontal, *pt* pterygoid, *q* quadrate, *qj* quadratojugal, *sq* squamosal, *st* supratemporal

supraoccipital. The cranial suture to the frontals is sinuous. Rostrolaterally, the parietal bears a recess that receives the caudal extension of the postfrontal. The caudal processes of the parietal diverge at right angles from the intertemporal bar, becoming more slender laterally and curving at their distal tip onto the medial face of the squamosals. On the laterocaudal corner of the skull, a laminar and laterome-dially elongated **supratemporal** extends from the lateral tip of the transverse process of the parietal to caudally overlap the dorsal margin of the squamosal.
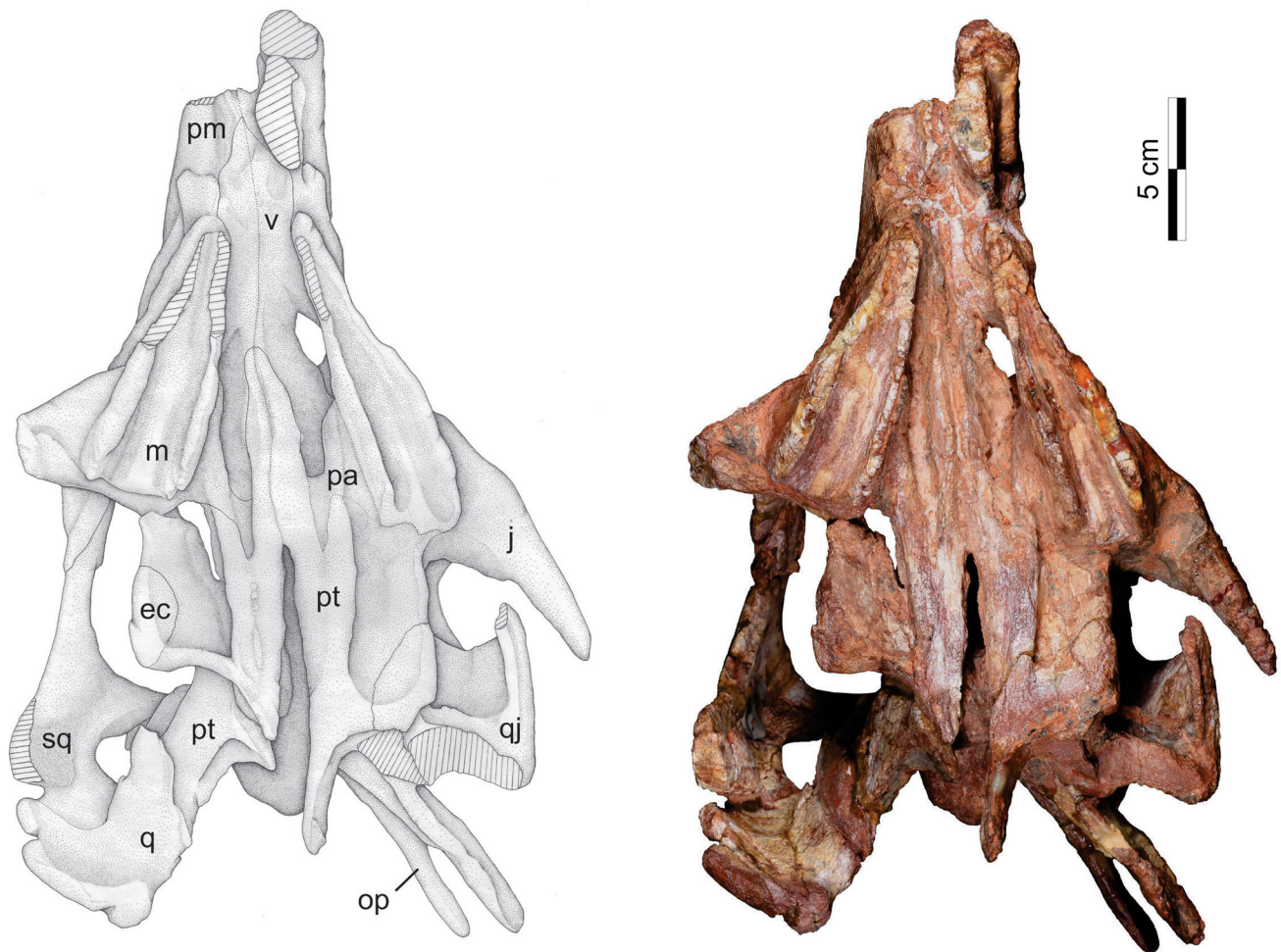
Fig. 5 *Brasinorhynchus mariantensis* (UFRGS-PV-0168-T; holotype). Drawing and photograph of the skull in ventral view. *ec* ectopterygoid, *j* jugal, *m* maxilla, *op* opistotic, *pm* premaxilla, *pt* pterygoid, *q* quadrate, *qj* quadratojugal, *sq* squamosal; *v* vomer

The **lachrymal** forms the rostral border of the orbit. Its contact with the prefrontal cannot be precisely defined, but its sutures with jugal and maxilla are seen in left lateral view. The former is V-shaped and the latter extends almost vertically along two-thirds of its length and then turns backwards at an angle of 45°. The **prefrontal** forms most of the slightly thickened dorsal margin of the orbit, meeting postfrontal, frontal, and nasal medially. The **postfrontal** is subtrianglar in shape. The medial side meets the frontal along a marked ridge, and its caudal tip is laterally bent, so that the parietal slots between frontal and postfrontal. The ventral ramus of the bone meets the postorbital, bridging the gap between the orbit and the upper temporal fenestra. The **postorbital** is better exposed in lateral view, an unusual feature among rhynchosaurs, given by the taller and narrower skull of *Brasinorhynchus mariantensis*. It bears a dorsoventrally tall, lateromedially compressed caudal process, the caudal tip of which is rounded. The ventral process forms an oblique contact with the jugal, at about the

mid-height of the orbit, forming its caudodorsal margin. The rostral and caudal processes contact, respectively, the postfrontal and the squamosal, and the latter forms the rostral part of the intertemporal bar.

The triradiate **jugal** occupies a significant portion of the cheek area. The wedge-shaped rostrodorsal ramus inserts between maxilla and lachrymal. At its tip, the continuation of the maxillary anguli oris crest extends obliquely along most of the lateral surface of the main body of this bone. Yet, the anguli oris crest does not expand along the rostrodorsal process of the jugal as in hyprodapedontine rhynchosaurs. There is no sign of foramina aligned ventral to that crest, as seen in other rhynchosaurs, but scattered foramina are seen above the crest. The caudodorsal ramus extends between the orbit and the lower temporal fenestra, and gets thinner as it extends below the postorbital. The ventrally arched caudoventral ramus is incomplete on either side. Yet, its strong lateroventral orientation suggests that it did not reach the quadratojugal. The medial surface
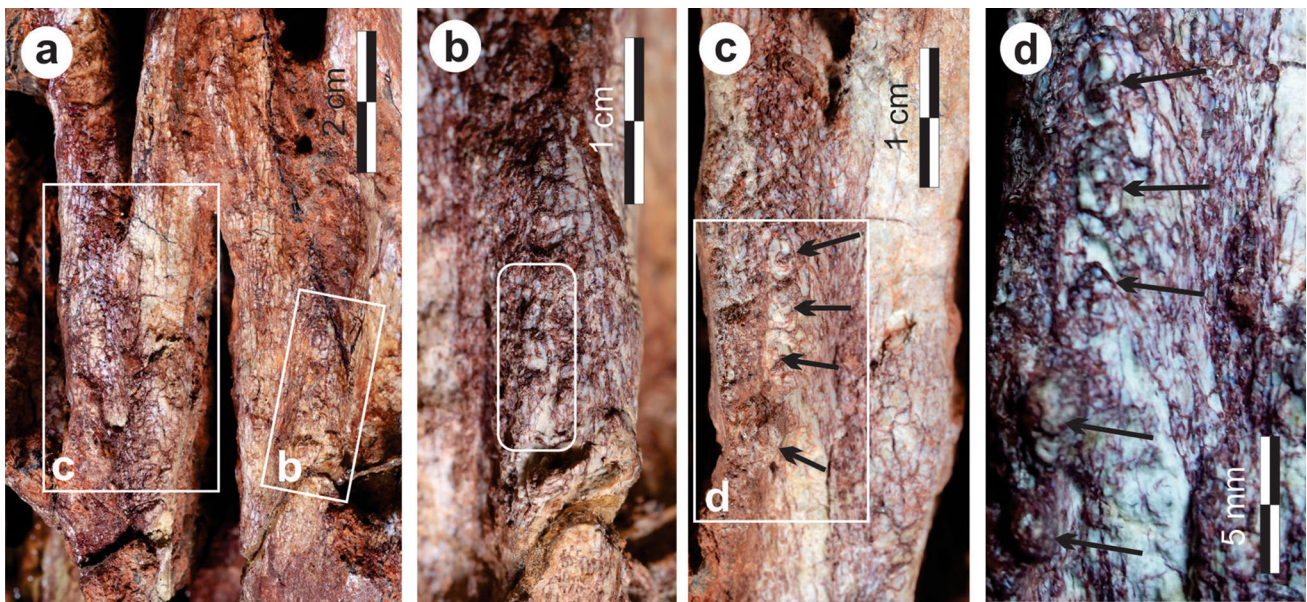
Fig. 6 *Brasinorhynchus mariantensis* (UFRGS-PV-0168-T; holotype). Photographs of the pterygoid teeth. **a** General view of the palatal area showing the areas highlighted in **b** and **c**; **b** ventral surface of the right pterygoid showing (*square*) area covered with "tooth material"; **c** ventral surface of the left pterygoid showing area highlighted in **d** and "tooth elements" (*arrows*); **d** ventral surface of the left pterygoid showing (*arrows*) "tooth elements"
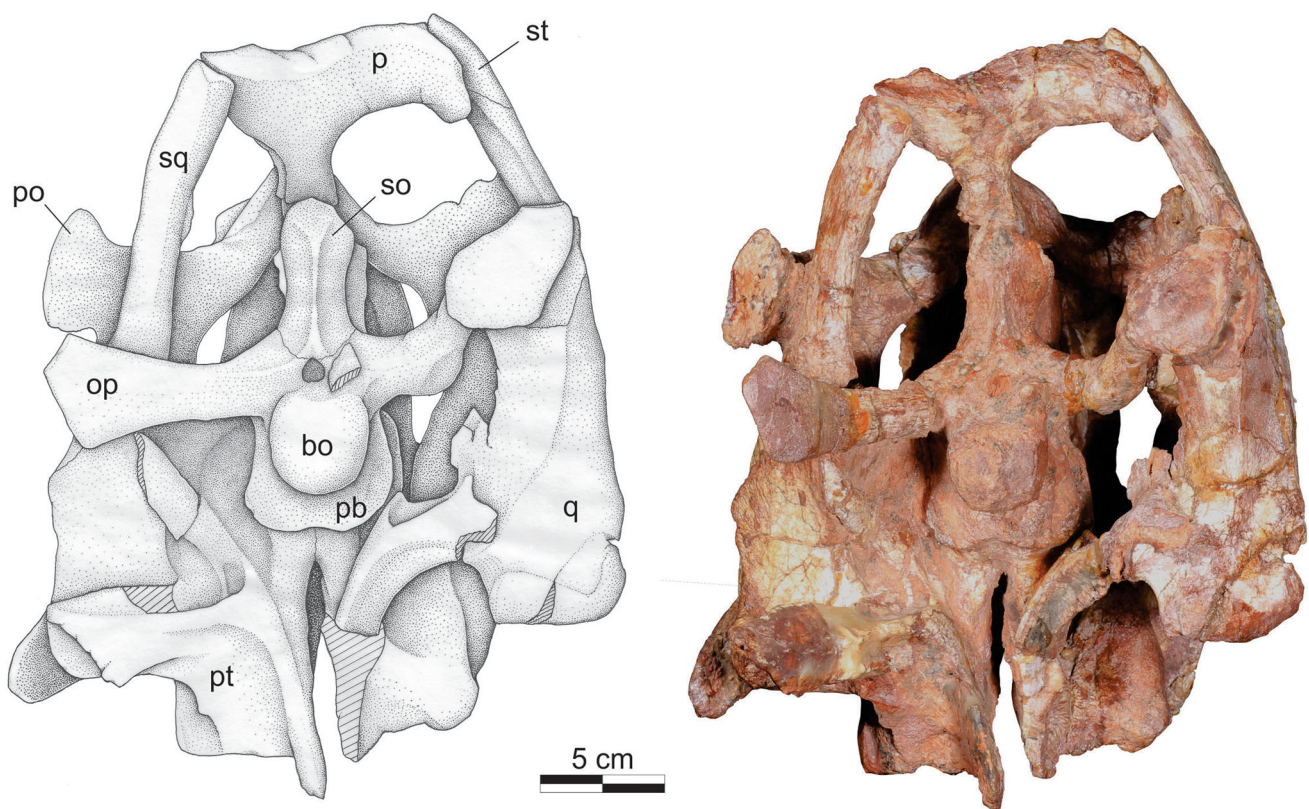

Fig. 7 *Brasinorhynchus mariantensis* (UFRGS-PV-0168-T; holotype). Drawing and photograph of the skull in occipital view. *bo* basioccipital, *pb* parabasisphenoid, *op* opistotic, *p* parietal, *po* postorbital, *pt* pterygoid, *q* quadrate, *so* supraoccipital, *sq* squamosal, *st* supratemporal
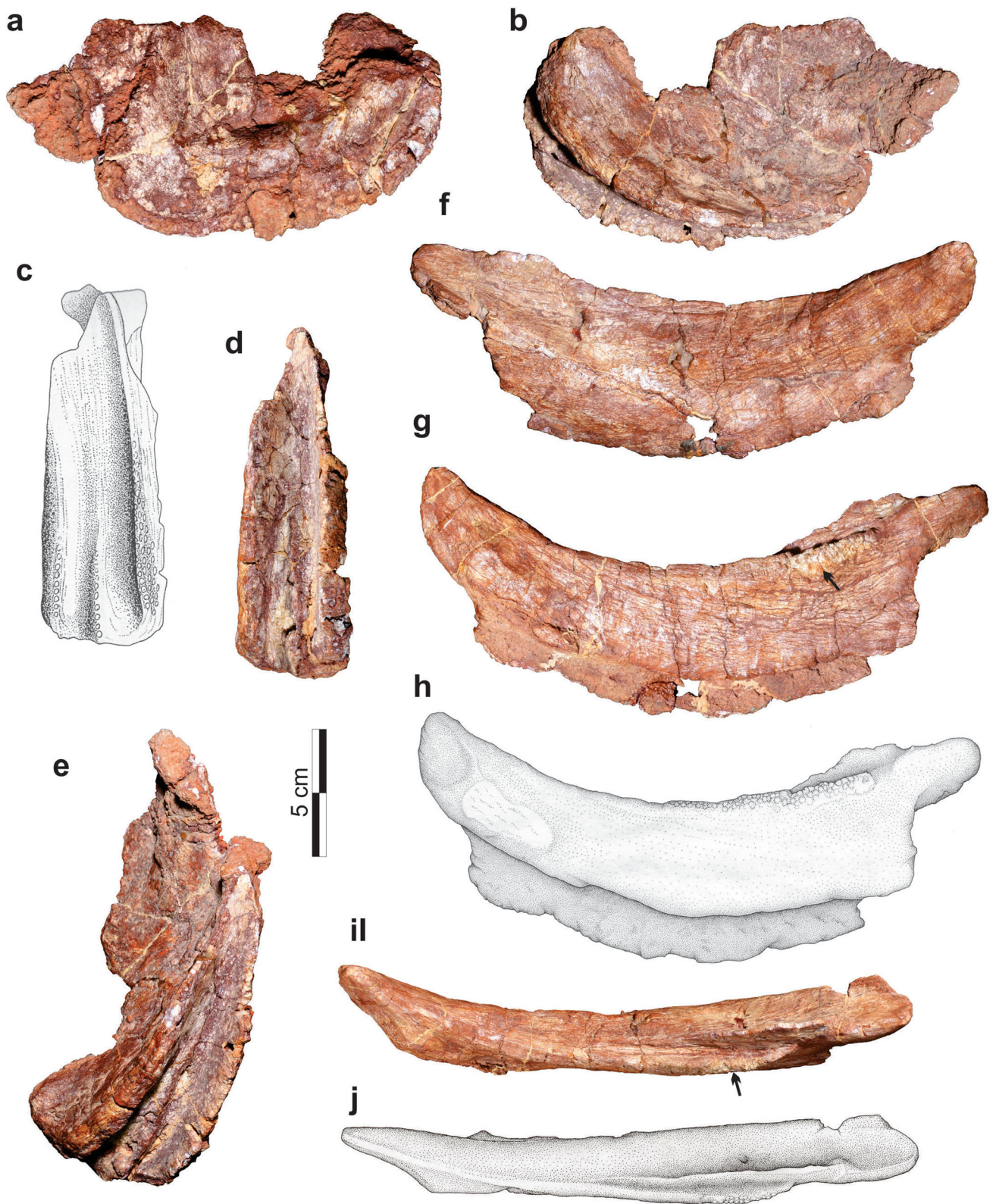
Fig. 8 *Brasinorhynchus mariantensis* (UFRGS-PV-0315-T), drawings and photographs of right tooth-bearing elements. **a–e** Maxilla in medial (**a**), lateral (**b**), occlusal (**c**, **d**), and lateroventral (**e**) views; **f–j**, dentary in lateral (**f**), medial (**g**, **h**), and occlusal (**i**, **j**) views. *Black arrow* indicates bulged area on the medial surface of the dentary
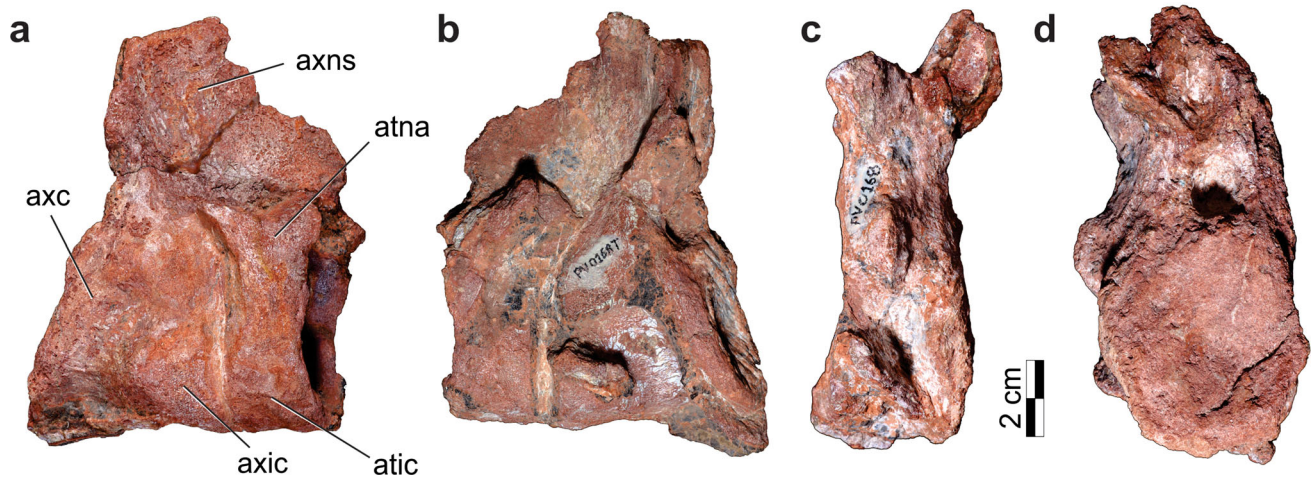
Fig. 9 *Brasinorhynchus mariantensis* (UFRGS-PV-0168-T; holotype), photographs of the preserved vertebrae. **a**, **b** Atlas-axis complex in right (**a**) and left (**b**) lateral views; **c**, **d** third cervical vertebra in left lateral (**c**) and caudal (**d**) views. *tic* atlantal intercentrum, *atna* atlantal neural arch, *axc* axial centrum, *axic* axial intercentrum, *axns* axial neural spine

of the jugal bears a central, vertical column, which attaches ventrally to the ectopterygoid.

The also triradiate **squamosal** is sub-vertically oriented and very deep. It forms the upper caudolateral corner of the skull and the caudolateral border of the upper temporal fenestra. The rostral ramus forms the intertemporal bar; it is flattened and laterally covered by the postorbital. The caudomedial ramus is also flattened, but curved and dorsocaudally overlaps the parietal wings. The ventral process bears a curved eminence that, at mid-high of the skull, fits to the upper border of the quadrate. From that point downwards, the ramus curves cranially to meet the lateral border of the quadrate and, more ventrally, the quadratojugal. This ramus narrows down, forming most of the caudal border of the lower temporal fenestra. The **quadratojugal** forms the lower caudolateral corner of the skull. It is a rather small bone if compared to those of the Late Triassic rhynchosaurs, and subtriangular in shape. Its upper wedge-shaped tip fits between the quadrate and the descending process of the squamosal. The caudal margin of the quadratojugal is firmly sutured to the quadrate, but its rostral portion is not completely preserved. It was probably moderately short and did not contact the caudoventral ramus of the jugal.

The vertical elongation of the **quadrate** is one of the most marked features of the much deeper skull in *B. mariantensis* if compared to other rhynchosaurs. Its ventral margin corresponds to the mandibular condyle, which takes the shape of a transversally elongated, medially broader hemi-cylinder, not forming a double articulation. Dorsal to the condyle, the quadrate bears a strong vertical pillar, slightly concave caudally. Two well-developed laminae extend lateral and medial to the pillar, the former of which is better developed. The lateral lamina meets

the quadratojugal and squamosal, whereas the medial reaches the quadrate ramus of the pterygoid.

The paired **vomers** form the palatal area between the premaxillae and the rostral part of the maxillae. Each bone has a small rostromedial process that meets its counterpart to form a wedge shaped element between the premaxillae. The rostral part of the vomers expands laterally to meet the maxillae in curved suture, forming the rostral margins of the choanae. Their caudal rami are elongated, reaching the caudal third of the rostrocaudal length of the maxillary occlusal surfaces, where they meet the pterygoids and apparently the palatines (at the caudomedial borders of the choanae). The joined caudal rami of the vomers form most of the interchoanal bar, each corresponding to a rounded crest separated by a deep groove, where the suture between the pairs is seen. A similar pattern extends caudally along the pterygoid, which forms the rest of the interchoanal bar. Each **palatine** is hourglass-shaped, its constricted portion forming the bone separation between the choana and the infraorbital fenestra. Its expanded portions meet the maxilla laterally and the pterygoid, and possibly the vomer, medially.

The **pterygoid** is a complex bone with two well-developed rami, termed the quadrate and ectopterygoid processes. The former extends caudolaterally and is much longer, following the rostrocaudal elongation of the skull. It corresponds to a lateromedially flattened bar that caudally overlaps the quadrate at its distal portion. The shorter ectopterygoid process extends laterally and is covered ventrally by the eponymous bone. The pterygoids are sutured medially at their rostral portion and diverge from one another caudal to that, but not as much as in other rhynchosaurids. Worn out teeth are seen at mid-length of the rostrocaudal axis of the main body of the pterygoids.

They are located caudomedially to the suborbital fenestra, slightly oblique (caudomedially to rostrolaterally) to the main axis of the bone. On the right side, five tooth elements have been recognized (Fig. 6). In occipital view, the deep basipterygoid processes of the parabasisphenoid fit into depressions on the dorsal surface of the pterygoids. The **ectopterygoid** connects the palate to the lateral portion of the skull roof, more specifically, the pterygoid to the maxilla. It covers the ectopterygoid ramus of the pterygoid, forms the caudal margin of the infraorbital fenestra, but a possible contact with the palatine is not visible. Medial to that, the rostral portion of the bone expands dorsally and is firmly attached to the caudal margin of the maxilla.

Matching the overall shape of the skull, the **supraoccipital** corresponds to a very deep bone, with a well-developed sagittal crest. Lateral to the crest, the bone extends rostrally and ventrally to meet other bones of the braincase. Dorsally, the supraoccipital fits into a slot in the broadened ventral portion of the intertemporal bar of the parietal. The suture with the exoccipital/opisthotic is not clear, and it is not possible to determine if the supraoccipital took part in the dorsal margin of the foramen magnum. In lateral view, it is possible to see that the rostral portion of the supraoccipital meets the prootic ventrally, via a straight suture. The paroccipital process of the **opisthotic** connects the braincase to the caudolateral corner of the skull roof (squamosal) as a deep bar. It forms an angle of about 45° to the sagittal line, so that the caudal margin of the braincase is well inset rostrally from the caudal margin of the skull. Both **epipterygoids** of *B. mariantensis* are preserved in their original positions, forming the rostrolateral margin of the braincase. It corresponds to a dorsoventrally elongated and lateromedially flattened bone. Its ventral portion is expanded rostrocaudally, whereas the narrower dorsal portion extends until near the ventral surface of the parietal.

The **basioccipital** forms the floor of the foramen magnum and a large spherical occipital condyle, slight flattened at its dorsal margin. The bone is constricted rostral to that, but expands again where the basal tubera are seen. The contact with the **parabasisphenoid** is not clearly seen. That bone is concave at its centre, forming a particularly depressed rounded area between the basal tubera. Rostral to that, well-developed basipterygoid processes extend ventrally in almost straight angles. These are subtriangular in shape and distally rounded where they meet the pterygoids. As preserved, the parasphenoid rostrum extends until the caudal margin of the maxillae, and is exceedingly deep.

The holotype skull lacks an articulated lower jaw, and only the **dentary** is known for UFRGS-PV-0315-T. It is not as deep as in most Late Triassic rhynchosaurs (Benton 1983a; Langer and Schultz 2000b). Its rostral tip is rather worn, but a single smooth crest is seen. As it extends caudally, this crest diverges medially, so that the oblique flattened area lateral to that is much more extensive than the medial, which extends to the vertical medial surface of the bone. The caudal half of the dentary crest is covered with small teeth and is medially flanked by a secondary and less prominent ridge placed in the middle (lateromedially) of the dentary, which does not extend along the rostral half of the bone. The lateral crest is lower than the medial at its rostral portion, but the opposite is seen more caudally. The lateral crest is narrower, bearing a single row of small, packed teeth along its apex. On the contrary, the broader medial crest bears various rows of small, packed teeth, that extend from the occlusal area to the lingual surface of the dentary.

The holotype skull was preserved along with three articulated **cervical vertebrae** (Fig. 9). Of the atlas, the rounded centrum (odontoid process), the cranially concave intercentrum, and the arches are preserved in the front of the atlas-axis block, but no further detail is seen. The axial intercentrum is similar in size to that of the atlas, and broader than its centrum. The later is rounded in cross section with a ventral keel extending along its ventral surface. Both of its articulations are slightly convex. The axial centrum lacks a well-defined parapophysis at the rostrolateral surface. The neural arch has a craniocaudally expanded neural spine and is as deep as the centrum. The third cervical vertebra bears no distinctive features worth describing.

Results and discussion

Phylogenetic analyses

The parsimony analysis retrieved two most parsimonious trees (Fig. 8) of 170 steps (CI 0.67, RI 0.75), both of which are mostly congruent with the phylogenetic hypotheses of Ezcurra et al. (2016). The South African forms *Mesosuchus browni*, *Howesia browni*, and *Eohyosaurus wolvaardti* form a paraphyletic array of successive sister groups to a monophyletic Rhynchosauridae. *Rhynchosaurus articeps* is the first diverging taxon within Rhynchosauridae and *Fodonyx spenceri* corresponds to sister taxon of a monophyletic Hyperodapedontinae. Defined as all taxa closer to *Hyperodapedon gordoni* than to *Fodonyx spenceri*, as modified from Langer and Schultz (2000b) to accommodate the new generic attribution of the latter species, Hyperodapedontinae includes the genera *Isalorhynchus*, *Teyumbaita*, and *Hyperodapedon*.

The major difference between the present hypothesis and that of Ezcurra et al. (2016) is the possible alternative positions of *Langeronyx brodiei* and *Bentonyx sidensis*. In the new analysis, *L. brodiei* is placed either as proposed by

Ezcurra et al. (2016) or more highly nested than *Bentonyx sidensis*, as the sister group of Hyperodapedontinae plus *Fodonyx spenceri* (Fig. 8). Two new characters correspond to synapomorphies of the clade seen in the alternative arrangement proposed here: the caudal orbital margin located caudal to the caudal margin of the maxillary tooth bearing area (character 101: 1 → 0) and maxillary lingual teeth extending to the rostral half of maxilla (character 111: 1 → 0).

Two major clades are recognized within Rhynchosauridae (Fig. 10): one congregating Mid-Late Triassic taxa at the branch leading to Hyperodapedontinae (i.e., *Bentonyx sidensis*, *Langeronyx brodiei*, *Fodonyx spenceri*, *Isalorhynchus genovefae*, *Teyumbaita sulcognathus*, and *Hyperodapedon* spp.) and the other (including *Brasinorhynchus mariantensis*) composed only of Middle

Triassic taxa. A branch-based definition for Stenaulorhynchinae was proposed as "all taxa closer to *Stenaulorhynchus stockleyi* than to *Hyperodapedon gordoni*" (Langer and Schultz 2000a). Its application to the recovered topology circumscribes *Ammorhynchus navajoi*, *Mesodapedon kuttyi*, *Stenaulorhynchus stockleyi*, and *Brasinorhynchus mariantensis*.

Stenaulorhynchinae is supported by the large number of maxillary lingual teeth on the medial surface of the bone (character 73: 0 → 1) and the reduced size of maxillary occlusal teeth, with each longitudinal row formed by a great number of elements (character 110: 0 → 1). The sister group relation between *S. stockleyi* and *B. mariantensis* is supported by the presence of three or more tooth rows medial to the main maxillary groove (character 70: 0 → 1). *Mesodapedon kuttyi* has been suggested to

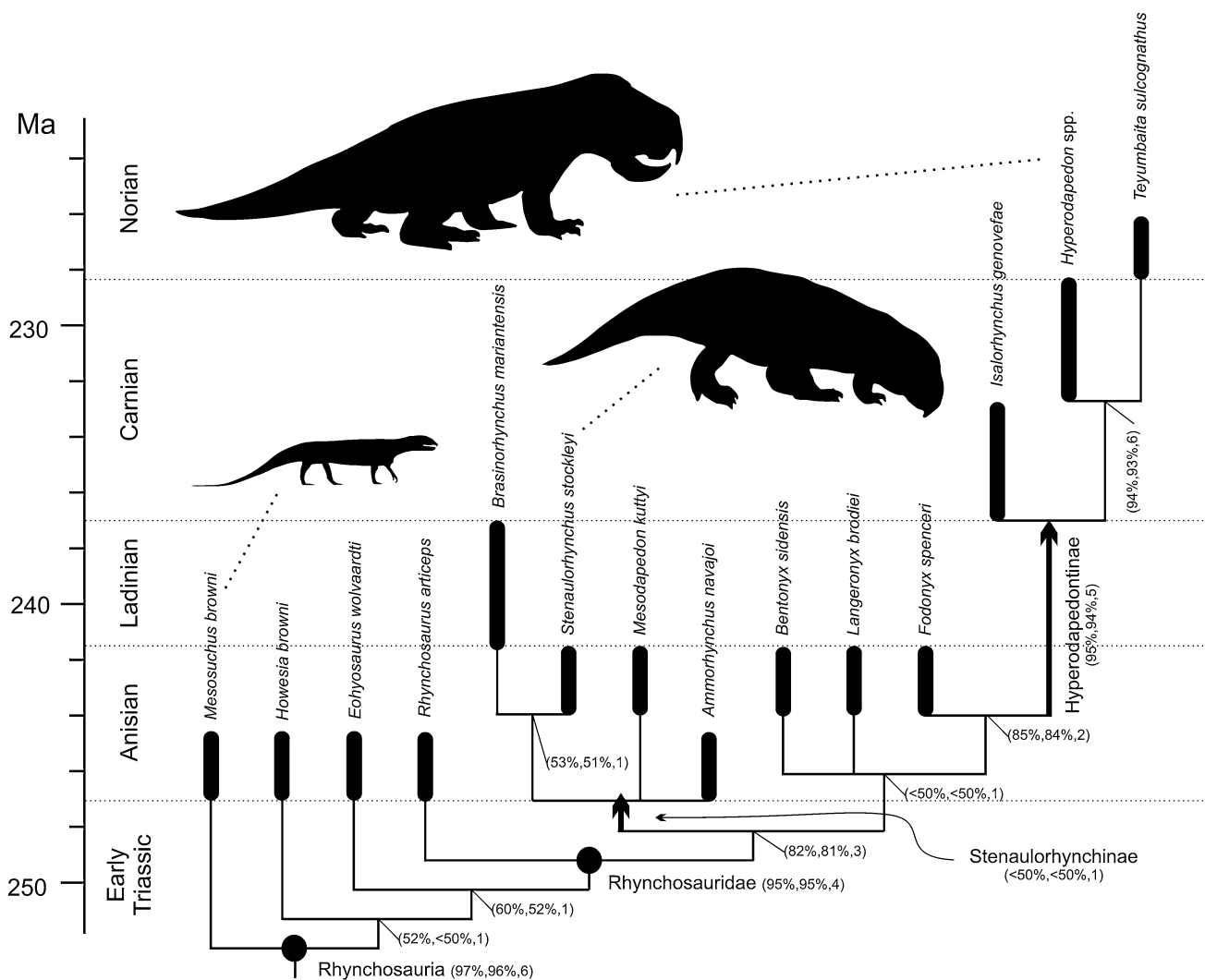**Fig. 10** Time-calibrated phylogenetic hypothesis for rhynchosaur relationships. Named branch- and node-based taxa are respectively indicated by *black arrows* and *circles*. Bootstrap absolute and GC values, as well as Bremer decay indices, are provided under brackets for each clade. *Black silhouettes* from different sources and nearly at the same scale. Timescale from Gradstein et al. (2012)

represent a junior synonym of *S. stockleyi* by Dilkes (1998). We regard both taxa as unique mainly due to their different provenance and scoring of character 70. In addition, a more conservative scoring of character 108, prevented resolving the basal polytomy of Stenaulorhynchinae. Yet, *M. kuttyi* shares with *S. stockleyi* and *B. mariantensis* two longitudinal grooves in the maxilla, suggesting a closer affinity among these three taxa. In addition, although not scored in the phylogentic analysis, maxillary tooth size and number of teeth per longitudinal row in *Ammorhynchus navajoi* seems intermediate between the conditions of the remaining Stenaulorhynchinae and their immediate outgroups. Further investigation and additional specimens are necessary for a better understanding of the affinities of *M. kuttyi* and *A. navajoi*.

The stenaulorhynchine clade is amongst the least supported in the study (bootstrap absolute and GC values of <50 % and Bremer decay index of 1). Accordingly, an exploratory analysis was conducted in order to test the validity of that clade and the characters supporting it. As missing data is known to cause poor support measurements, even when the positions of taxa are stable (Wilkinson 2003; Siddall 2002; Prevosti and Chemisquy 2010), we removed the two most fragmentary forms, *Ammorhynchus navajoi* and *Mesodapedon kuttyi*, from the data set and reran the analysis. The same MPTs (167 steps, CI 0.68, RI 076) were recovered and the topologies are fully congruent with the first analysis. In this second analysis, the *Brasinorhynchus mariantensis* + *Stenaulorhynchus stockleyi* clade shows better support indices (Bremer decay index: 5, Absolute Bootstrap frequency: 86 %, GC Bootstrap frequency: 83 %). Support measures calculated from pruning *A. navajoi* and *M. kuttyi* from the first analysis resulted in similar values (Bremer decay index 5, Absolute Bootstrap frequency: 85 %, GC Bootstrap frequency 82 %). In addition, the clade is supported by a greater number of synapomorphies: presence of a well-marked 'V'-shaped crest along the frontal-postfrontal contact, rostral to the margin of the supratemporal fossa (character 25: $0 \rightarrow 1$); distal tip of the transverse process of the parietal rostroventrally curved (character 38: $0 \rightarrow 1$); presence of a large number of maxillary lingual teeth on the medial surface of the bone (character 73: $0 \rightarrow 1$); crowded teeth on the dentary lingual surface (character 80: $0 \rightarrow 1$); prefrontal and postfrontal closer to, or contacting one another, reducing the participation of the frontal in dorsal orbital border (character 103: $0 \rightarrow 1$); caudal portion of the medial surface of the dentary forming a bulged area that projects medially (character 106: $0 \rightarrow 1$; Fig. 8); and reduced size of maxillary occlusal teeth, with each maxillary longitudinal row formed by great number of teeth (character 110: $0 \rightarrow 1$). Among the synapomorphies recovered in the exploratory analysis, the derived states of

characters 25, 38, and 103 are unique to *B. mariantensis* + *S. stockleyi* clade, but could not be scored for *A. navajoi* and *M. kuttyi*, given their fragmentary nature. The study of the two more complete stenaulorhynchines, *B. mariantensis* and *S. stockleyi*, highlights their peculiar anatomy within Rhynchosauria, but a better understanding of *A. navajoi* and *M. kuttyi* is needed for a more complete assessment of the evolutionary patterns of this enigmatic clade of Middle Triassic rhynchosaurs.

Stenaulorhynchines (and other rhynchosaurs) in space and time

The grouping of four taxa into a novel rhynchosaur clade (Stenaulorhynchinae) deserves a macroevolutionary contextualization. The record of *Rhynchosaurus articeps* in the Anisian of England (Benton et al. 1994; Ezcurra et al. 2016) indicates that, during that time, rhynchosaurs quickly expanded their occurrence range from South Africa to other parts of Pangea, as the early Anisian rocks of the Burgersdorp Formation (*Cynognathus* Assemblage Zone, Subzone B), in the Karroo Basin, yielded all non-Rhynchosauridae rhynchosaurs known to date (Butler et al. 2015; Ezcurra et al. 2016). In turn, Stenaulorhynchines correspond to a further radiation, still mainly constrained to the Mid-Triassic (Figs. 10, 11). From the early Anisian Moenkopi Formation of northern Arizona (Nesbitt and Whatley 2004), *Ammorhynchus navajoi* is the only known northern component of that event, whereas *Stenaulorhynchus stockleyi*, *Mesodapedon kuttyi*, and *Brasinorhynchus mariantensis* indicate a more diverse and somewhat younger Gondwanan radiation. The former two taxa, found respectively in the Manda beds and Yerrapalli Formation, are considered of late Anisian age (Abdala and Ribeiro 2010), whereas *B. mariantensis* is the only definite stenaulorhynchine with a likely younger distribution.

Although a strong age calibration of the tetrapod Assemblage-Zones of the Brazilian Triassic is lacking (Langer et al. 2007; Abdala et al. 2009), evidence for Anisian-aged deposits are meager. This includes the stenaulorhynchine affinity of *Brasinorhynchus mariantensis* itself (Schultz 1995) and isolated records of the traversodontid *Luangwa* (Abdala and Sá-Teixeira 2004), a genus first known in the Anisian Upper Ntawere Formation of Zambia (Abdala and Ribeiro 2010). Yet, there is evidence, both in Brazil (Da Silva and Cabreira 2009) and Namibia (Abdala et al. 2013), of younger (Ladinian) records of *Luangwa*. Accordingly, until stronger evidence comes to light, global data better support a Ladinian age for all Middle Triassic rocks of the Santa Maria Formation. On the contrary, new radioisotopic data suggests that at least part of those deposits is Late Triassic in age. Philipp et al. (2013) provided a U–Pb maximum age of 236 Ma from
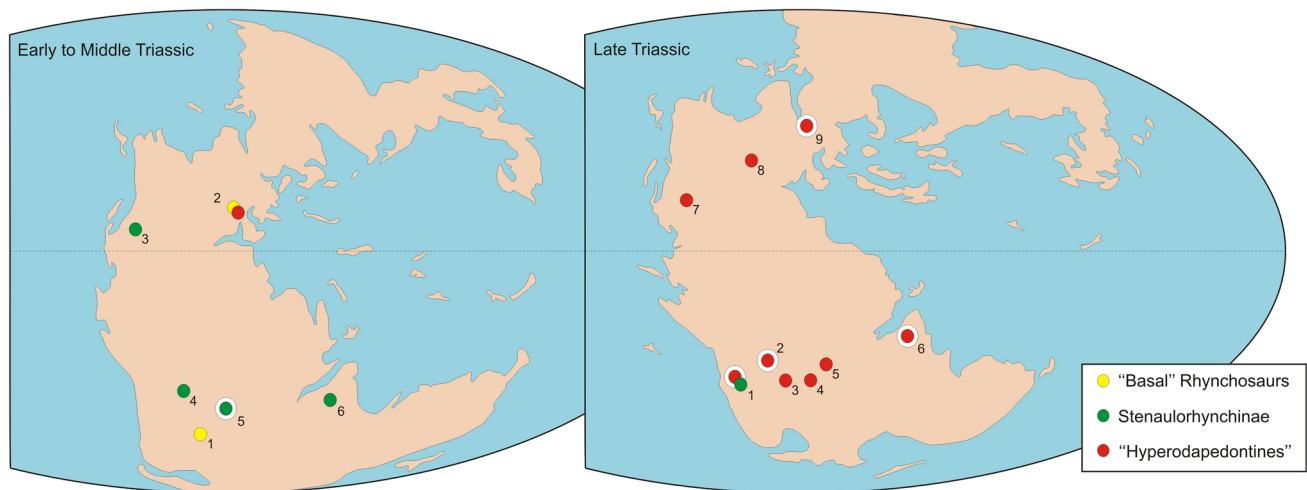
Fig. 11 Paleogeographic distribution of rhynchosaurs (maps from R. Blakey, Mollewide plate tectonic maps, http://jan.ucc.nau.edu/rcb7/mollglobe.html). Early to Middle Triassic map: *1* South Africa; *2* English midlands; *3* western USA; *4* Rio Grande do Sul, Brazil; *5* Tanzania; *6* peninsular India. Late Triassic map: *1* northwestern Argentina; *2* Rio Grande do Sul, Brazil; *3* Zimbabwe; *4* Tanzania; *5* Madagascar; *6* peninsular India; *7* western USA; *8* Nova Scotia; *9* Scotland. *White contours* indicate faunas with high rhynchosaur abundance

detrital zircons recovered from the middle portion of the Santa Cruz sequence of the Santa Maria Formation (Horn et al. 2014). This sequence roughly corresponds to the *Santacruzodon* Assemblage Zone (Abdala et al. 2001; Soares et al. 2011), which has been traditionally considered Ladinian in age and correlated to the Triassic deposits of the Isalo II beds, in Madagascar, that yielded the rhynchosaur *Isalorhynchus genovefae*, among other taxa (see below). Similarly, the Chañares Formation in Argentina, until recently considered typically Ladinian (Lucas, 1998; Abdala and Ribeiro 2010; but see Desojo et al. 2011), has been given a maximum U–Pb age of 236 Ma (Marsicano et al. 2015). Accordingly, both the Chañares fauna and the *Santacruzodon* AZ fit into the early Carnian of more recent time scales (Gradstein et al. 2012; Mietto et al. 2012). Hence, pending on the discovery of more complete remains, the recently found rhynchosaurs from the Chañares Formation (Ezcurra et al. 2013), which may be a second South American stenaulorhynchine, suggests a somewhat delayed expansion of the group to the western border of Gondwana. As for *Brasinorhynchus marianten-sis*, both its biostratigraphic (=*Dinodontosaurus* AZ; Lucas 2001; Langer et al. 2007; Abdala et al. 2009, 2013) and sequence stratigraphy (=Pinheiros-Chiniquá Sequence; Horn et al. 2014) provenances suggest that it is older than the maximally 236 Ma old *Santacruzodon* AZ and Santa Cruz sequence. Accordingly, Ladinian is probably still the best age estimate for the taxon.

In ecological terms, stenaulorhynchines are commonly minor components of their faunas. This is the case of *Ammorhynchus navajoi*, *Brasinorhynchus mariantensis*, *Mesodapedon kuttyi*, and the Chañares form, all represented

only by a handful of specimens in faunas with a rather extensive record of other terrestrial tetrapods (Bandyopadhyay et al. 2002; Nesbitt 2005; Abdala et al. 2013; Fiorelli et al. 2013). In contrast, the English Mid-Triassic is not particularly well sampled for tetrapods (Benton et al. 1994), and the relative abundance of rhynchosaurs may be preservation biased. Accordingly, it seems that *Stenaulorhynchus stockleyi*, from the Manda Beds of Tanzania, has been the only rhynchosaur to attain a certain faunal dominance during the Middle Triassic (Benton 1983b; Ezcurra et al. 2016).

The sister lineage to Stenaulorhynchinae has a mirroring evolutionary history (Figs. 10, 11). The clade is not diverse in the Middle Triassic, represented only by *Bentonyx sidensis*, *Fodonyx spenceri*, and *Langeronyx brodiei*, from the late Anisian of England (Benton et al. 1994). Yet, it includes most Late Triassic rhynchosaurs, the Hyperodapedontinae, the diversity increase of which may be correlated to the demise of stenaulorhynchines, in the context of a still poorly understood faunal turnover across the Ladinian-Carnian boundary. Moreover, hyperodapedontines are well represented in various Late Triassic faunas (Langer et al. 2000; Lucas and Heckert 2002), as highlighted by the dominance of *Hyperodapedon* in the Tiki and Upper Maleri formations, peninsular India (Mukherjee and Ray 2014), Lossiemouth Sandstone Formation, Scotland (Benton and Walker 1985), *Hyperodapedon* Acme-Zone of the Santa Maria Formation, south Brazil (Langer et al. 2007), and lower Ischigualasto Formation, Argentina (Martínez et al. 2013). The *Hyperodapedon*-dominated beds of the latter unit have been dated as 231.4 ± 0.3 Ma (Martínez et al. 2011), i.e., late Carnian (Gradstein et al., 2012), an age that could be extended to

the above mentioned Indian, Scottish, and Brazilian faunas with a similar ecological scenario. Other Gondwanan records of *Hyperodapedon* come from not so well sampled faunas from Tanzania and Zimbabwe (Langer et al. 2000), where the dominance of the genus cannot be confirmed, although its occurrence suggests a late Carnian age. In North America, *Hyperodapedon* was recorded in the Middle Wolfville Formation, Nova Scotia, and the Popo Agie Formation, Wyoming (Lucas et al. 2002). There is evidence that both of these units may be of late Carnian age (Langer 2005; Leleu and Hartley 2010; Butler et al. 2014), i.e., older than the dated Late Triassic tetrapod-rich strata of the Chinle Formation (Irmis et al. 2011; Ramezani et al. 2014). Indeed, the lack of rhynchosaurs in the Chinle Formation, instead of indicating an uneven rhynchosaur distribution, is most probably age constrained, and representative of a condition that postdates the diversity peak of these archosauromorphs over Pangea. Isolated humeri distal ends from the Bull Canyon Formation of New Mexico, USA, were recently referred to Rhynchosauria (Spielmann et al. 2013). Yet, as with the specimens previously attributed to *Otischalkia elderae* (Hunt and Lucas 1991; see Long and Murry 1995; Montefeltro et al. 2013), the new material lacks rhynchosaur diagnostic features, and cannot be promptly assigned to the group.

Records of the monospecific genera *Isalorhynchus* and *Teyumbaita* bracket the range of the cosmopolitan *Hyperodapedon*. *Isalorhynchus genovefae* is known from the base of the "Isalo II" beds of Besairie (1972; =Makay Formation; Razafimbelo 1987), in Madagascar. As discussed by many authors (Flynn et al. 2000, 2010; Abdala and Ribeiro 2010; Kammerer et al. 2010; Nesbitt et al. 2015), these beds may predate the *Hyperodapedon*-dominated faunas, probably corresponding to the early Carnian, as corroborated by the radioisotopic age of the likely coeval *Santacruzodon* Assemblege Zone in Brazil (Philipp et al. 2013). Conversely, *Teyumbaita sulcognathus* appears to be the last surviving rhynchosaur. Its records are consistently above those of *Hyperodapedon* in south Brazil (Langer et al. 2007; Montefeltro et al. 2010), largely suggesting a Norian age.

References

Abdala, F., and A.M. Ribeiro. 2010. Distribution and diversity patterns of Triassic cynodonts (Therapsida, Cynodontia) in Gondwana. *Palaeogeography, Palaeoclimatology, Palaeoecology* 286: 202–217.

Abdala, F., and A.M. Sá-Teixeira. 2004. A traversodontid cynodont of African affinity in the South American Triassic. *Palaeontologia Africana* 40: 11–22.

Abdala, F., A.M. Ribeiro, and C.L. Schultz. 2001. A rich cynodont fauna of Santa Cruz do Sul, Santa Maria Formation (Middle-Late Triassic), southern Brazil. *Neues Jahrbuch für Geologie und Paläontologie Monatshefte* 11: 669–687.

Abdala, F., A.G. Martinelli, M.B. Soares, M. de la Fuente, and A.M. Ribeiro. 2009. South American Middle Triassic continental faunas with amniotes: biostratigraphy and correlation. *Palaeontologia Africana* 44: 83–87.

Abdala, F., C.A. Marsicano, R.M. Smith, and R. Swart. 2013. Strengthening Western Gondwanan correlations: a Brazilian Dicynodont (Synapsida, Anomodontia) in the Middle Triassic of Namibia. *Gondwana Research* 23: 1151–1162.

Andreis, R. R., G.E. Bossi, and D.K. Montardo. 1980. O Grupo Rosário do Sul, Triássico no Rio Grande do Sul. In *Anais do XXXI Congresso Brasileiro de Geologia*. 2: 659–673. Camboriú, Siciedade Brasileira de Geologia.

Bandyopadhyay, S., T.K. Roy Chowdhury, and D.P. Sengupta. 2002. Taphonomy of some Gondwana vertebrate assemblages of India. *Sedimentary Geology* 147: 219–245.

Benton, M.J. 1983a. The Triassic reptile *Hyperodapedon* from Elgin: functional morphology and relationships. *Philosophical Transaction of the Royal Society B* 302: 605–717.

Benton, M.J. 1983b. Dinosaur success in the Triassic: a noncompetitive ecological model. *The Quarterly Review of Biology* 58: 29–55.

Benton, M.J., and A.D. Walker. 1985. Palaeoecology, taphonomy, and dating of Permo-Triassic reptiles from Elgin, north-east Scotland. *Palaeontology* 28: 207–234.

Benton, M.J., G. Warrington, A. Newell, and P.S. Spencer. 1994. A review of the British Mid Triassic tetrapod faunas. In *In the Shadow of the Dinosaurs*, ed. N.C. Fraser, and H.-D. Sues, 131–160. New York: Columbia University.

Besairie, H. 1972. Géologie de Madagascar I. Les terraines sédimentaires. *Annales Géologiques de Madagascar, Service des Mines* 35: 1–463.

Brazeau, M. 2011. Problematic character coding methods in morphology and their effects. *Biological Journal of the Linnean Society* 104: 489–498.

Bremer, K. 1994. Branch support and tree stability. *Cladistics-the International Journal of the Willi Hennig Society* 10: 295–304.

Butler, R.J., O.W.M. Rauhut, M.R. Stocker, and R. Bronowicz. 2014. Redescription of the phytosaurs *Paleorhinus* ("*Francosuchus*") *angustifrons* and *Ebrachosuchus neukami* from Germany, with implications for Late Triassic biochronology. *Zoological Journal of the Linnean Society* 170: 155–208.

Butler, R., M. Ezcurra, F. Montefeltro, A. Samathi, and G. Sobral. 2015. A new species of basal rhynchosaur (Diapsida: Archosauromorpha) from the early Middle Triassic of South Africa, and the early evolution of Rhynchosauria. *Zoological Journal of the Linnean Society* 174: 571–588.

Chatterjee, S. 1980. The evolution of rhynchosaurs. *Mémoires de la Société géologique de France* 139: 57–65.

Da Rosa, A.A.S. 2014. Geological context of the dinosauriform-bearing outcrops from the Triassic of Brazil. *Journal of South American Earth Sciences* 61: 108–119.

Da Silva, L.R., and S.F. Cabreira. 2009. Novo achado de *Luangwa sudamericana* Abdala & Teixeira, 2004 do Triássico Médio da Formação Santa Maria, Rio Grande do Sul, Brasil. *Palaeontologia em Destaque* 24: 23–24.

Desojo, J.B., M.D. Ezcurra, and C.L. Schultz. 2011. An unusual new archosauriform from the Middle-Late Triassic of southern Brazil and the monophyly of Doswelliidae. *Zoological Journal of the Linnean Society* 161: 839–871.

Dilkes, D. 1998. The Early Triassic rhynchosaur *Mesosuchus browni* and the interrelationships of basal archosauromorph reptiles. *Philosophical Transactions of the Royal Society of London Series B-Biological Sciences* 353: 501–541.

Ezcurra, M.D., M.J. Trotteyn, L.E. Fiorelli, M.B. von Baczko, J.R.A. Taborda, M. Iberlucea, and J.B. Desojo. 2013. The oldest rhynchosaur from Argentina: a Middle Triassic rhynchosaurid from the Chañares Formation (Ischigualasto–Villa Unión Basin, La Rioja Province). *Paläontologische Zeitschrift* 88: 453–460.

Ezcurra, M.D., F.C. Montefeltro, and R.J. Butler. 2016. The early evolution of rhynchosaurs. *Frontiers in Ecology and Evolution* 3: 142.

Fiorelli, L.E., M.D. Ezcurra, E.M. Hechenleitner, E. Argañaraz, J.R.A. Taborda, M. Jimena Trotteyn, M.B. von Baczko, and J.B. Desojo. 2013. The oldest known communal latrines provide evidence of gregarism in Triassic megaherbivores. *Scientific Reports* 3: 3348.

Flynn, J.J., J.M. Parrish, L. Ranivoharimanana, W.F. Simpson, and A.R. Wyss. 2000. New traversodontids (Synapsida: Eucynodontia) from the Triassic of Madagascar. *Journal of Vertebrate Paleontology* 20: 422–427.

Flynn, J.J., S.J. Nesbitt, J.M. Parrish, L. Ranivoharimanana, and A.R. Wyss. 2010. A new taxon of *Azendohsaurus* (Archosauromorpha, Diapsida, Reptilia) from the Triassic Isalo Group of southwest Madagascar: part 1, cranium. *Palaeontology* 53: 669–688.

Goloboff, P., J. Farris, and K. Nixon. 2008. TNT, a free program for phylogenetic analysis. *Cladistics* 24: 774–786.

Gradstein, F.M., J.G. Ogg, M.D. Schmitz, and G.M. Ogg. 2012. *The Geologic Time Scale 2012*, 1144. Oxford: Elsevier.

Horn, B.L.D., T.P. Melo, C.L. Schultz, R.P. Philipp, H.P. Kloss, and K. Goldberg. 2014. A new third-order sequence stratigraphic framework applied to the Triassic of the Paraná Basin, Rio Grande do Sul, Brazil, based on structural, stratigraphic and paleontological data. *Journal of South American Earth Sciences* 55: 123–132.

Hunt, A.P., and S.G. Lucas. 1991. A new rhynchosaur from West Texas (USA) and the biochronology of Late Triassic rhynchosaurs. *Palaeontology* 34: 927–938.

Irmis, R.B., R. Mundil, J.W. Martz, and W.G. Parker. 2011. High-resolution U–Pb ages from the Upper Triassic Chinle Formation (New Mexico, USA) support a diachronous rise of dinosaurs. *Earth and Planetary Science Letters* 309: 258–267.

Kammerer, C.F., J.J. Flynn, L. Ranivoharimanana, and A.R. Wyss. 2010. The first record of a probainognathian (Cynodontia: Chiniquodontidae) from the Triassic of Madagascar. *Journal of Vertebrate Paleontology* 30: 1889–1894.

Langer, M.C. 2005. Studies on continental Late Triassic tetrapod biochronology. II. The Ischigualastian and a Carnian global correlation. *Journal of South American Earth Sciences* 19: 219–239.

Langer, M.C., and C.L. Schultz. 2000a. Rincossauros- herbívoros cosmopolitas do Triássico. In *Paleontologia do Rio Grande do Sul*, ed. M. Holz, and L.F. Roz, 246–272. Porto Alegre: CIGO/UFRGS.

Langer, M.C., and C.L. Schultz. 2000b. A new species of the late Triassic rhynchosaur *Hyperodapedon* from the Santa Maria Formation of south Brazil. *Palaeontology* 43: 633–652.

Langer, M.C., M. Boniface, G. Cuny, and L. Barbieri. 2000. The phylogenetic position of *Isalorhynchus genovefae*, a Late Triassic rhynchosaur from Madagascar. *Annales de Paléontologie* 86: 101–127.

Langer, M.C., A.M. Ribeiro, C.L. Schultz, and J. Ferigolo. 2007. The continental tetrapod–bearing Triassic of South Brazil. *Bulletin of the New Mexico Museum of Natural History and Science* 41: 201–218.

Leleu, S., and A.J. Hartley. 2010. Controls on the stratigraphic development of the Triassic Fundy Basin, Nova Scotia: implications for the tectonostratigraphic evolution of Triassic. *Journal of the Geological Society, London* 167: 437–454.

Long, J.A., and P.A. Murry. 1995. Late Triassic (Carnian and Norian) tetrapods from the Southwestern United States. *Bulletin of the New Mexico Museum of Natural History and Science* 4: 1–254.

Lucas, S.G., and A.B. Heckert. 2002. The *Hyperodapedon* Biochron, Late Triassic of Pangea. *Albertiana* 27: 30–38.

Lucas, S.G. 1998. Global Triassic tetrapod biostratigraphy and biochronology. *Palaeogeography, Palaeoclimatology, Palaeoecology* 143: 347–384.

Lucas, S.G. 2001. Age and correlation of Triassic tetrapod assemblages from Brazil. *Albertiana* 26: 13–20.

Lucas, S.G., A.B. Heckert, and N. Hotton III. 2002. The rhynchosaur *Hyperodapedon* from the upper Triassic of Wyoming and its global biochronological significance. *Bulletin of the New Mexico Museum of Natural History and Sciences* 21: 149–156.

Marsicano, C.A., R.B. Irmis, A.C. Mancuso, R. Mundil, and F. Chemale. 2015. The precise temporal calibration of dinosaur origins. In *Proceedings of the National Academy of Science* Online first.

Martínez, R.N., P.C. Sereno, O.A. Alcober, C.E. Colombi, P.R. Renne, I.P. Montañez, and B.S. Currie. 2011. A basal dinosaur from the dawn of the dinosaur era in southwestern Pangaea. *Science* 331: 206–210.

Martínez, R.N., C. Apaldetti, O.A. Alcober, C.E. Colombi, P.C. Sereno, E. Fernandez, P.S. Malnis, G.A. Correa, and D. Abelin. 2013. Vertebrate succession in the Ischigualasto Formation. *Journal of Vertebrate Paleontology* 32: 10–30.

Mietto, P., et al. 2012. The global boundary stratotype section and point (GSSP) of the Carnian Stage (Late Triassic) at Prati di Stuores/Stuores Wiesen section (southern Alps, NE Italy). *Episodes* 3: 414–430.

Montefeltro, F., M.C. Langer, and C.L. Schultz. 2010. Cranial anatomy of a new genus of hyperodapedontine rhynchosaur (Diapsida, Archosauromorpha) from the upper Triassic of southern Brazil. *Earth and Environmental Science Transactions of the Royal Society of Edinburgh* 101: 27–52.

Montefeltro, F., J. Bittencourt, M.C. Langer, and C.L. Schultz. 2013. Postcranial anatomy of the hyperodapedontine rhynchosaur *Teyumbaita sulcognathus* (Azevedo and Schultz, 1987) from the Late Triassic of southern Brazil. *Journal of Vertebrate Paleontology* 33: 67–84.

Mukherjee, D., and S. Ray. 2014. A new *Hyperodapedon* (Archosauromorpha, Rhynchosauria) from the upper Triassic of India: implications for rhynchosaur phylogeny. *Palaeontology* 57: 1241–1276.

Nesbitt, S. 2005. Stratigraphy and tetrapod fauna of major quarries in the Moenkopi Formation (Early-Middle Triassic) along the Little Colorado River of northern Arizona. *Bulletin of the Mesa Southwest Museum* 11: 18–33.

Nesbitt, S.J., and R.L. Whatley. 2004. The first discovery of a rhynchosaur from the upper Moenkopi Formation (Middle Triassic) of northern Arizona. *PalaeoBios* 24: 1–10.

Nesbitt, S.J., J.J. Flynn, A.C. Pritchard, J.M. Parrish, L. Ranivoharimanana, and A.R. Wyss. 2015. Postcranial osteology of *Azendohsaurus madagaskarensis* (?Middle to Upper Triassic, Isalo Group, Madagascar) and its systematic position among stem archosaur reptiles. *Bulletin of the American Museum of Natural History* 398: 1–126.

Philipp, R.P., H. Closs, C.L. Schultz, M. Basei, B.L.D. Horn, and M.B. Soares. 2013. Proveniência por U-Pb LA-ICP-MS em zircão detrítico e idade de deposição da Formação Santa Maria, Triássico da Bacia do Paraná, RS: evidências da estruturação do Arco do Rio Grande. In *Anais do VIII Symposium International on Tectonics & XIV Simpósio Nacional de Estudos Tectónicos*, 154–157. Cuiabá.

Prevosti, F., and M. Chemisquy. 2010. The impact of missing data on real morphological phylogenies: influence of the number and distribution of missing entries. *Cladistics* 26: 326–339.

Ramezani, J., D.E. Fastovsky, and S.S. Bowring. 2014. Revised chronostratigraphy of the lower Chinle Formation strata in Arizona and New Mexico (USA): high-precision U-Pb geochronological constraints on the Late Triassic evolution of dinosaurs. *American Journal of Science* 314: 981–1008.

Razafimbelo, E. 1987. *Le basin de Morondava (Madagascar). Synthèse géologique et structurale*. Ph.D. dissertation. Strasbourg, Université Louis Pasteur. p. 189.

Schultz, C.L. 1995. Subdivisão do Triássico do RS com base em macrofósseis: problemas e perspectivas. *Comunicações do Museu de Ciências e Tecnologia, UBEA/PUCRS, Série Ciências da Terra* 1: 25–32.

Schultz, C.L., and S.A.K. Azevedo. 1990. Dados preliminares sobre a ocorrência de uma nova forma de rincossauro para o Triássico do Rio Grande do Sul-Brasil. *Paula-Coutiana* 4: 35–44.

Siddall, M.E. 2002. Measures of support. In *Techniques in molecular systematics and evolution*, ed. R. DeSalle, G. Giribet, and W.C. Wheeler, 80–101. Basel: Birkhauser Verlag.

Soares, M.B., C.L. Schultz, and B.L.D. Horn. 2011. New information on *Riograndia guaibensis* Bonaparte, Ferigolo & Ribeiro, 2001 (Eucynodontia, Tritheledontidae) from the Late Triassic of southern Brazil: anatomical and biostratigraphic implications. *Anais da Academia Brasileira de Ciências* 83: 329–354.

Spielmann, J.A., S.G. Lucas, and A.P. Hunt. 2013. The first Norian (Revueltian) rhynchosaur: Bull Canyon Formation, New Mexico, USA. *New Mexico Museum of Natural History and Science Bulletin* 61: 562–566.

Wilkinson, M. 2003. Missing entries and multiple trees: instability, relationships, and support in parsimony analysis. *Journal of Vertebrate Paleontology* 23: 311–323.

Zerfass, H., E.L. Lavina, C.L. Schultz, A.G.V. Garcia, U.F. Faccini, and F. Chemale Jr. 2003. Sequence stratigraphy of continental Triassic strata of southernmost Brazil: a contribution to Southwestern Gondwana palaeogeography and palaeoclimate. *Sedimentary Geology* 161: 85–105.